Matrix Mechanosensing: From Scaling Concepts in 'Omics Data to Mechanisms in the Nucleus, Regeneration, and Cancer

Dennis E. Discher,[1] Lucas Smith,[1] Sangkyun Cho,[1] Mark Colasurdo,[2] Andrés J. García,[2] and Sam Safran[3]

[1]Molecular and Cell Biophysics Lab, University of Pennsylvania, Philadelphia, Pennsylvania 19104; email: discher@seas.upenn.edu

[2]Parker H. Petit Institute for Bioengineering and Biosciences, Georgia Institute of Technology, Atlanta, Georgia 30332

[3]Department of Materials and Interfaces, Weizmann Institute of Science, Rehovet 76100, Israel

Keywords

polymer physics, collagen, lamins, myosin, contractility

Abstract

Many of the most important molecules of life are polymers. In animals, the most abundant of the proteinaceous polymers are the collagens, which constitute the fibrous matrix outside cells and which can also self-assemble into gels. The physically measurable stiffness of gels, as well as tissues, increases with the amount of collagen, and cells seem to sense this stiffness. An understanding of this mechanosensing process in complex tissues, including fibrotic disease states with high collagen, is now utilizing 'omics data sets and is revealing polymer physics–type, nonlinear scaling relationships between concentrations of seemingly unrelated biopolymers. The nuclear structure protein lamin A provides one example, with protein and transcript levels increasing with collagen 1 and tissue stiffness, and with mechanisms rooted in protein stabilization induced by cytoskeletal stress. Physics-based models of fibrous matrix, cytoskeletal force dipoles, and the lamin A gene circuit illustrate the wide range of testable predictions emerging for tissues, cell cultures, and even stem cell–based tissue regeneration. Beyond the epigenetics of mechanosensing, the scaling in cancer of chromosome copy number variations and other mutations with tissue stiffness suggests that genomic changes are occurring by mechanogenomic processes that now require elucidation.

Contents

INTRODUCTION

Polymer physics has successfully focused for more than half a century on properties that are independent of detailed chemistries (36). Cell and tissue functions have rarely been explained in terms of polymer physics even though the solid-like nature of tissues is due to polymers, particularly proteins, and most tissue cells are anchorage dependent in that viability requires adhesion to a solid (35). For mammals the most abundant protein is the structural protein outside of cells, collagen 1, which can self-assemble in water into macroscopic fibers and solidified networks or gels with a stiffness that depends on concentration. Thus, the sensitivity of cells to matrix stiffness might seem a logical consequence of anchorage dependence, but stiffness sensing has become a topic of great interest as well as some controversy.

From another perspective, the chemistry of a cell's surroundings is often sensed by a cell, particularly the specific type and concentration of a ligand to which a cell receptor might bind. From the overwhelming accumulation of molecular biology data, it is perhaps tempting to believe that molecular detail is needed to explain all cell biological responses, with cells sensing only the precise chemical details of their microenvironments. However, mammalian cells clearly exhibit an acute sensitivity to at least one physical variable of the environment, namely temperature. Every cell science lab sets their incubators at a physiological 37°C rather than, for example, 47°C, which would fry cells. The temperature of the surrounding medium propagates into a cell and, indeed, regulates conformational probabilities and pathway fluxes, even regulating gene expression via inducible transcription factors (79). The softness or stiffness of the surroundings to which a cell adheres likewise seems to be sensed, propagated, and transduced into conformational and biochemical changes within a cell, some of which are reviewed here.

CORRELATED EXPRESSION OF STRUCTURAL BIOPOLYMERS: MINING 'OMICS OF THREE-DIMENSIONAL TISSUES

For synthetic polymers, theory and basic experiments have advanced our understanding sufficiently to guide the widespread use and generation of many polymer types, mixtures, and composites.

Structural polymer systems generally sustain stresses and strains even at a scale much smaller than a cell, and synthetics in everyday use are sometimes soft or rubbery but others are hard and resist cracking. For biopolymers with structural roles in hydrated native tissues, such as collagens outside cells or cytoskeletal components inside cells, disorder is often evident and mysteries abound concerning any relationship(s) between composition, order of architecture, and microscopic physical properties.

Proteomics, transcriptomics, genomics, and other emerging 'omics can perhaps offer insight as these methods provide increasingly reproducible and accessible data sets about the relative concentrations of specific proteins and nucleic acid species in various complex tissues with native matrix and multiple cell types. Mining such data sets, derived from three-dimensional (3D) functional tissues, for correlations rooted in polymer physics can perhaps illustrate an emerging means for generating initial hypotheses for reductionist studies of mechanisms (**Figure 1**). Transcriptome databases, in particular, are standardized for many tissues, especially the US National Institutes of Health's GEO database (Gene Expression Omnibus; **https://www.ncbi.nlm.nih.gov/geo/**). However, a top-down perspective should first seek to relate a collective physical property, such as the stiffness of a tissue, to its protein composition.

On the micron length scale relevant to a cell, the tissue stiffness is a microelasticity, E (or Young's modulus), that is measured in units of stress (kPa). For numerous tissues, E has been measured by various labs using diverse methods, and the magnitude of E spans at least two to three logs, from soft brain or marrow to the very stiff osteoid that bone-forming osteoblasts remodel into bone (as summarized in 25). Bone is a good example of a tissue with very large differences in microscopic versus macroscopic mechanics: The microelasticity of osteoid is $\sim$20–50 kPa whereas the macroscopic rigidity of bone is approximately a gigapascal (i.e., 10^6 kPa). Such log scale variations are crucial to identifying any polymer physics–based trends (36). As an example, recent mass spectrometry–based proteomics studies of adult mouse tissue (80), indeed, indicate a typical, nonlinear polymer physics–type of scaling relationship for each of the two collagen 1 gene products, *Col1a1* and *Col1a2* (**Figure 2a**), which co-assemble stoichiometrically to make collagen 1 protein:

$$E \sim \text{collagen 1}^n \text{ with } n \approx 0.67.$$

In such scaling relations, prefactors with units of (stiffness/density^n) are ignored, as are small (but important) offsets that represent the critical concentrations needed to percolate a network. Similar magnitude exponents, n, are found for other fibrillar collagens, including collagens 3, 5, 6, 11, and 12, making it clear that higher levels of fibrillar collagen are found in stiffer tissues (e.g., cardiac and skeletal muscle or bone-forming osteoid). Enzymatic degradation can be used to decrease the concentration of fibrils in a tissue or tumor (25), or cross-linking can be used to solidify fibril interactions, and both processes generally change tissue stiffness even for a soft embryonic tissue, such as heart (55). Importantly, power-law scaling of tissue stiffness with the concentration of these most abundant of structural biopolymers is overall consistent with the physical properties of polymer networks. Indeed, gels of pure collagen 1 have exponents (n) that decrease from $n = 2.8$ at 22°C to $n = 2.1$ at 37°C (89), or that weaken to $n \approx 1$ when the gels are under stress (51).

Beyond the fibrillar collagenous matrix in tissues, mass spectrometry–based proteomic profiling of more than 100 of the most abundant proteins in adult mouse tissues revealed few other proteins that also scaled with stiffness (80). A key exception is the nucleoskeletal protein lamin A (**Figure 2b**), which is an intermediate filament protein (like keratins in hair, hooves, and fingernails) that assembles beneath the nuclear envelope and that scales with tissue stiffness:

$$\text{lamin A} \sim E^m \text{ with } m \approx 0.7.$$
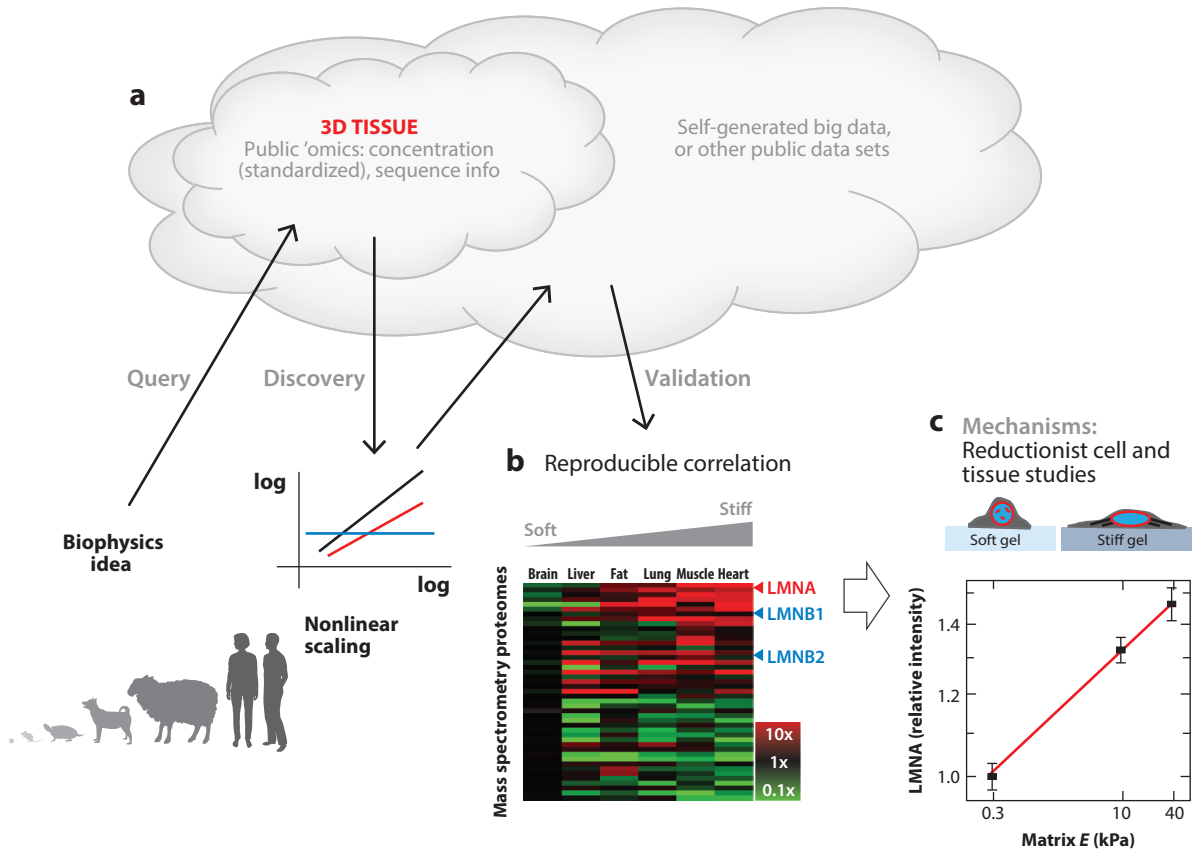
Figure 1

Tissue-based hypothesis development and testing in the Big Data Era. (*a*) Beginning with an idea rooted in biophysics, such as tissue stiffness increasing with tissue levels of the abundant biopolymer collagen 1, one can query publicly available 'omics data sets for three-dimensional (3D) tissue and seek out other factors that correlate with collagen 1. Such data sets are standardized and provide relative concentrations or sequence information, or both. Scaling relations as power laws in log–log plots would be particularly sensible for relationships between polymers, given collagen as an implicit expression of stiffness. The sketched plot illustrates, for example, a gene expression data set in which two genes increase in relative level when plotted against the relative level of a third gene, whereas one gene remains relatively constant. Self-generated 'omics data or other public data sets, or both, can provide a test of the scaling relationship. (*b*) Reproducible correlations across 'omics analyses might agree, for example, with an increase in lamin A (LMNA) from soft tissue (brain) to stiff tissue (heart), whereas the B-type lamins (LMNB1 and LMNB2) remain constant, as detected by quantitative mass spectrometry (80). (*c*) To understand molecular mechanisms for such relationships, reductionist approaches include low dimensionality and sparse cultures on 2D gels of controlled stiffness that are coated equally with collagen 1 for cell adhesion. With such systems, studies of mesenchymal stem cells show that lamin A increases (in relative intensity) from soft gels to stiff gels, with mechanisms involving cytoskeletal stress on the nucleus stabilizing lamin A against phosphorylation and degradation (10).

Typically, nuclei do not contribute much to tissue stiffness, and so this scaling relation quantifies the upregulation of A-type lamins (by up to 30-fold from soft brain to rigid bone) as part of a putative mechanoresponse to tissue stiffness, as elaborated in the section titled Nuclear Linkages and Forces in Gene Regulation. B-type lamin levels remain relatively constant: For lamin B1, $m \sim 0.2$, and for lamin B2, $m \sim 0.0$. Phylogenetic analyses have indicated that lamin B1 is the most ancient of intermediate filament proteins (e.g., keratins, vimentin, desmin) (26), and so one possible explanation of the different scaling exponents is that m evolved to achieve greater
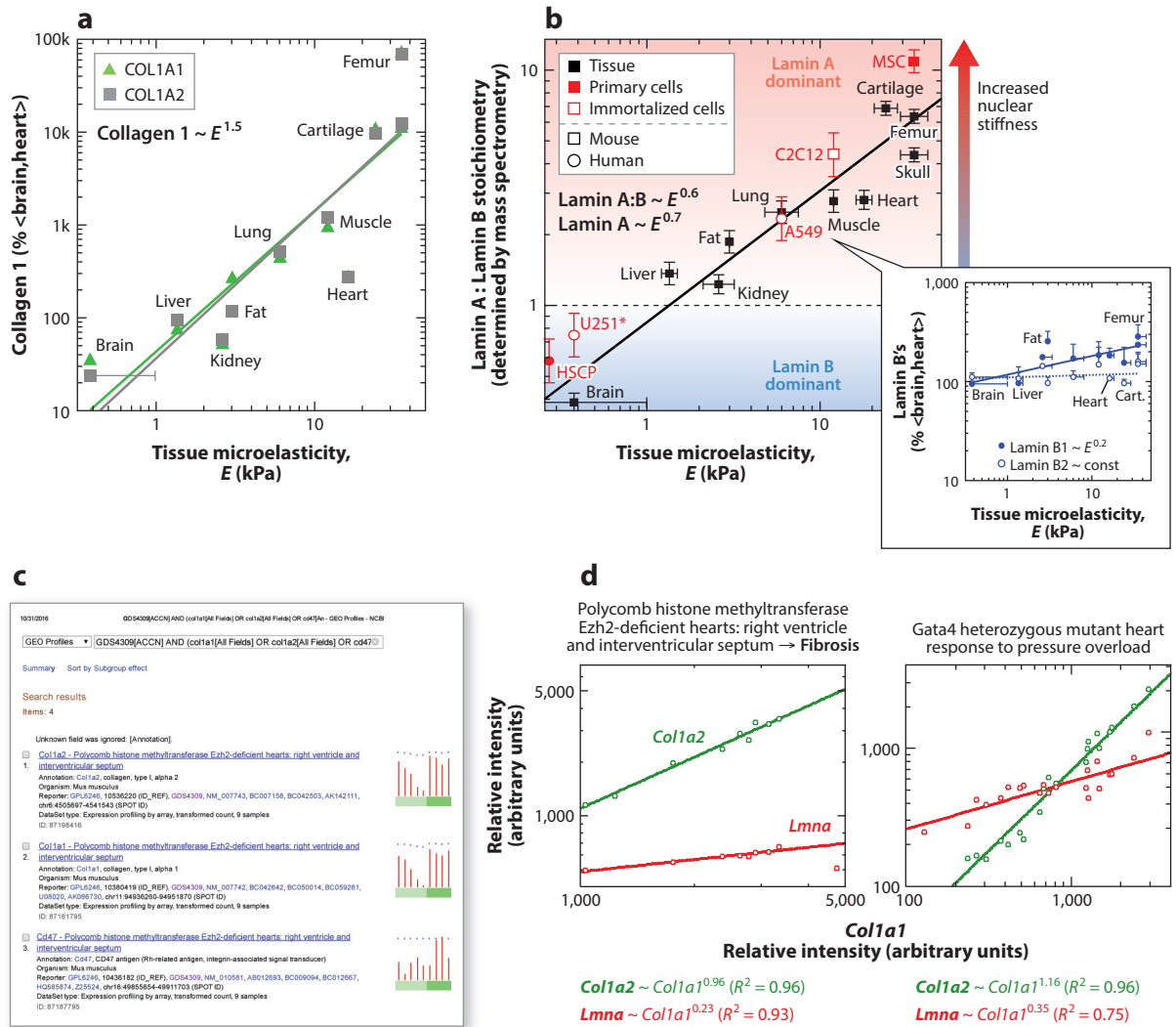
Figure 2

Scaling of collagen 1 and lamin A proteins with cell-scale tissue stiffness compared with transcriptome data mined for similar scaling relationships. (*a,b*) As measured with a variety of microtools at the scale of cells, tissue microelasticity or stiffness increased by two orders of magnitude for various species tested (see references in 80). For bones such as femur and skull, the stiffness of precalcified bone (called osteoid) is plotted. As a reference, a gummy bear is approximately 70 kPa. Quantitative mass spectrometry done on mouse tissue was used to determine the relative amounts of collagen 1 subunits. The two subunits exhibited similar scaling on the log–log plot because they form a stoichiometric complex as they assemble into collagen 1 fibers. The average level for heart and brain tissue was defined as 100%. For the lamins quantified in the same studies, lamin A (LMNA) is normalized to the B-type lamins (LMNB1 and LMNB2) that remain relatively constant across tissues. Nuclear stiffness increases with lamin A and, hence, with tissue stiffness. (*c*) A screen snapshot from the public transcriptome database GEO (Gene Expression Omnibus, accessible via the US National Institutes of Health at **https://www.ncbi.nlm.nih.gov/geo/**) shows the expression of *Col1a2* (*top*) in nine different mouse hearts and *Col1a1* (*middle*) in the same hearts. A similar pattern of expression is evident between these two, whereas *Cd47* (*bottom*) is a miscellaneous gene that exhibits a very different pattern of expression among samples. (*d*) Plots of *Col1a2* against *Col1a1* for such data sets reveal a linear scaling consistent with stoichiometric association at the protein level. Lamin A transcript (*Lmna*) also scales with *Col1a1*, but the scaling is much weaker with a log–log slope of approximately 0.3 across these two data sets from mouse hearts. Such weak scaling of mRNA is consistent with the weak scaling of protein, as can be deduced from panels *a* and *b*.

mechanosensitivity for lamin A while eliminating the mechanosensitivity of lamin B2. Until a suitable experiment such as in directed evolution is conducted, caution is needed for such discussions of evolution because most proteins, including lamins, serve multiple functions that could also be key determinants of optimizing tissue levels of lamins. Thus, collagens and other proteins of the extracellular matrix (ECM) set the stiffness of the tissue, and lamin A responds at the nuclear envelope. Because lamin A confers nuclear stability and stiffness [i.e., viscosity $\sim$ [lamin A]$^{2.5}$, which is typical of high polymers (80)], cells in stiffer, mechanically stressed tissues normally end up with stiffer and stronger nuclei.

Rearranging the scaling relations above gives the compositional correlation

$$\text{lamin A} \sim \text{collagen } 1^{\alpha} \text{ with } \alpha_{\text{Lmna}} = m \times n \approx 0.45,$$

which is a convenient form because these two factors are often reported in a wide range of expression studies, including most transcriptomic data sets. Causality must be established, of course, by in-depth cell biology studies, but similar robust trends might at least be sought in many other publicly available, standardized 'omics data sets.

As an example of a broad meta-analysis in today's Big Data Era, we focused initially on heart tissue. Heart offers the largest number of transcriptomic data sets of normal and diseased states relevant to mechanosensation, with open-access data sets available for normal development and aging, as well as fibrosis, myocardial injury, and hypertrophy. Data sets also span a wide range of species, including mouse, human, rat, boar, dog, and zebra fish (2, 16, 83). Once a data set is selected, a first check on quality is provided by collagen 1's two stoichiometric subunits: If *Col1a1* increases or decreases in level, then *Col1a2* should do the same in proportion. Changes in *Col1a1* between samples in a data set could be due to experimental perturbation, normal variation, or even experimental noise in other components of the analysis (**Figure 2c**). However, provided one finds for a given data set a reasonable fit ($R^2 > 0.85$) of the form

$$Col1a2 \sim Col1a1^{\alpha} \text{ with } \alpha_{Col1a2} = 1.0 \pm 0.2,$$

then the data set can be considered to pass a first validation. Importantly, public data are often provided in log form, and so even simple, linear statistical metrics such as the Pearson correlation coefficient between log levels of two transcripts can be a first indication of a relationship that might be rooted in polymer physics.

Transcript data from a mouse knockout model with fibrosis (23, 62) is plotted in log–log form versus *Col1a1* (**Figure 2d**). A strong positive correlation between *Col1a2* and *Col1a1* has a suitable slope ($\alpha_{Col1a2} = 0.96$) and goodness of fit ($R^2 = 0.96$), which provides some validation for further analysis. In comparison, *Lmna* increases more weakly ($\alpha_{Lmna} = 0.23$; $R^2 = 0.93$), which is consistent with the weak scaling in proteomics described above and supports a model wherein increased deposition of collagenous ECM results in higher levels of lamin A. A second data set from another group illustrates similar scaling (**Figure 2d**) (7), and so do most of the other GEO data sets on heart tissue, which yield an average scaling of $\alpha_{Lmna} = 0.3$ (16); some of the largest deviations (within ± 0.3) from this scaling occur when collagen subunit scaling is far from unity or poorly fit, or both. Although such positive scaling of transcripts does not prove causality, as emphasized above, the implied stiffness-dependent scaling of lamin A begins to suggest a general model of mechanotransduction from the ECM to the nucleus that is perhaps generalizable to a broader range of cell types and tissue and organ systems. Indeed, human muscular dystrophy shows a similar trend (see **Supplemental Figure 1**; follow the **Supplemental Material link** from the Annual Reviews home page at **http://www.annualreviews.org**), with increased collagen attributable to fibrosis, which is consistent with increased stiffness of dystrophic tissue (24).

SIMPLEST SIGNATURE OF MATRIX MECHANOSENSING: 2D CELL SPREADING

Collagen 1 is both an adhesion ligand and a structural protein. A tissue with high collagen is thus likely to present more adhesive ligand to a cell in such a tissue. The evident scaling relation between lamin A and collagen 1 could therefore reflect a purely biochemical signal from ligand density rather than any implicit dependence on tissue stiffness, E. It is difficult to separate such variables with intact tissue. However, many reductionist in vitro experiments with various materials allow separate control over adhesion ligand and substrate elasticity E, showing that cells mechanosense E as long as the ligand is not limiting.

The simplest experimental signature for mechanosensing substrate E is a saturable increase of cell spread area as a function of E with the stiffest possible gels and rigid glass causing similar cell spreading as soon as a few hours and certainly after one day (e.g., 29, 30, 64). Importantly, for any given gel or substrate, the amount of adhesive ligand (e.g., gelatin or nonfibrillar collagen) should be widely varied, but the usual observation is that beyond a threshold in the density of such ligand, the cell spread area increases asymptotically to a maximum spread area as a function of E. Inhibition of myosin II suppresses such spreading, and so actomyosin forces increase with E. It is also useful and important to vary the thickness of soft gels bound to rigid glass, because for gels that are only a few microns thick or less, cells are seen to spread (9, 10, 30). This is because the cell's actomyosin-driven distortions of the soft gels are constrained by the rigidity of the hidden, underlying glass. This latter approach maintains ligand biochemistry as well as gel physics and reveals the basic stiffness-sensing capabilities of adherent cells. It also highlights the need for careful attention to physical heterogeneity in culture systems because cells generally respond to rigid objects that are microns away (24).

A simple intuition into mechanosensing of matrix E is obtained by considering that actin polymerization drives cell spreading at a near constant rate, $v_{polymer} = A$, whereas myosin II pulls back on the actin network. The latter occurs at a rate of $v_{retract} = B/(K+E)$ that follows the usual hyperbolic decrease (with constants B, K) as a function of resistance set by the extracellular load; in this case, the load is E that the cells engage via integrins and perhaps other adhesion receptors. As with muscle, contraction and retraction rate is low at high loads. The extent of cell spreading relates to a steady state $v_{polymer} - v_{retract} = A - B/(K+E)$ that yields minimal cell spreading for $E \ll K$ and maximal spreading for $E \gg K$, which are limits widely observed for nearly all adherent cells (e.g., 29, 30, 64). A typical value for $K \sim 5$ kPa multiplied by a typical cell-generated strain of ~5% yields an estimate—through Netwon's third law—of the typical actomyosin contractile stress of approximately hundreds of pascals generated within a cell protrusion. Assuming a typical protrusion curvature radius of ~1 μm, such a stress can also be converted by the well-known Laplace law to an effective cortical tension of ~0.1 mN/m. A cortical tension of ~0.1 mN/m has indeed been measured for some cells, and this tension decreases dramatically with myosin II inhibition (74).

TISSUE STIFFNESS MEASUREMENTS

Because alterations in the ECM can alter mechanosensing by cells (19), it is important to measure tissue mechanical properties on fresh samples. Bulk measurement methods include rheometry, with standard mechanical properties reported as elastic modulus, shear, or bulk modulus; the viscoelastic nature of soft tissue is characterized at times by viscosity, stress relaxation, and creep. However, the length scales of strains and stresses produced by bulk methods are much greater than the few micrometers that a cell can apply forces to and sense. Atomic force microscopy (AFM) has enabled the mechanical characterization of fresh tissue on the cellular scale (44). The high spatial

resolution is able to decipher the high degree of mechanical heterogeneity in tissues that individual cells sense. The basic mode of action of AFM is indentation of a substrate with measurement of the force applied from the bending of an AFM cantilever. The Hertz model or a related model is fit to the resulting force indentation curve to extract material stiffness. Although AFM has provided an abundance of elastic modulus data at a cellular scale, it is important to remember that AFM is primarily used for indentation, and tensile properties can differ (57). Differences in indentation versus extension can be critical to understanding whether cells push or pull on their associated ECM and whether it is normal or diseased.

COLLAGEN PERTURBATION: FIBROSIS AND MECHANOSENSING

Fibrosis is the pathological accumulation of ECM, particularly fibrillar collagens, within any tissue, and it is associated with wound-healing processes that culminate in scars. Given the association of fibrosis with a wide array of tissue injuries, fibroproliferative disease is a global health burden, accounting for nearly 50% of deaths in the developed world either directly or indirectly (87). Altered mechanosensing from the progressively stiffening, fibrotic ECM is responsible both for the impaired ability of healthy cells to regenerate functioning tissue and for promoting the activation of fibroblasts to secrete even more ECM components (13).

Healthy lung has a stiffness of <5 kPa, but in fibrosis this increases to >15 kPa (8), with corresponding increases observed in fibrotic liver (22), striated muscle (78), and kidney (47). Although collagen concentration is a major component of stiffness, explaining rheological measurements of collagen gels requires additional properties (72). In terms of the rescaled bending modulus $\tilde{\kappa} = \kappa/\mu l^2$, where κ is the collagen fiber bending modulus, μ is the collagen fiber stretching modulus, and l is the lattice spacing, the stiffness of the collagen network is represented by K:

$$\frac{\tilde{\kappa}}{|\Delta\gamma|^\phi} \frac{K}{|\Delta\gamma|^f} \left(\pm 1 + \frac{K^{1/f}}{|\Delta\gamma|} \right)^{(\phi - f)}, \qquad 1.$$

with an inflection point at a critical strain γ_c used in $\Delta\gamma = \gamma - \gamma_c$. This critical strain is where the network transitions from floppy to rigid, with more highly connected networks becoming rigid at smaller strains. The branch ($\pm$) also depends on $\gamma \lessgtr \gamma_c$. Network rigidity scales linearly with protein concentration if the collagen fibers are elastic and it is relatively independent of fiber size (72). However, quantifying these parameters in tissues remains a challenge. Thus, although some measurements suggest that the extent of fibrosis does not correlate well with stiffness (76), collagen cross-linking, which is related to network connectivity, can have strong effects on mechanical properties, as shown in the fibrotic heart (53). Indeed, collagen cross-linking and the enzymes responsible for cross-linking are signatures of fibrotic disease (77) and provide therapeutic potential across many fibrotic conditions (3). Intriguingly, the ECM of cancerous tissue also becomes heavily cross-linked, leading to increased stiffness and oncogenic mechanosensing, with cross-linking inhibitors showing therapeutic promise (50).

Fibrotic tissue also has a high degree of heterogeneity. For example, the reticular pattern in idiopathic lung fibrosis is complex (18), with focal regions of increased stiffness measured by AFM in mouse models (52). The heterogeneity of fibrotic scars in otherwise soft tissue has been mimicked by copolymerizing polyacrylamide with collagen 1, which segregates into fibrous patches (24). The culture system has been used to show that mechanoresponsive cells are greatly affected by even a small and stiff fibrotic patch.

Fibrous collagen networks can be locally aligned by cellular contraction, which results in a high degree of strain-stiffening behavior in these networks (84). This can be modeled by breaking down the stress into components, $\sigma = \sigma_i + \sigma_f$, where σ_i represents the isotropic component of

the network, which depends on the initial bulk and shear moduli. And σ_f represents the fibrous component, which stiffens only in the direction of strain and depends on the initial modulus of the fibrous phase, the strain-hardening exponent, and the strain at which the fibers become aligned. In vitro experiments show that collagen is compacted and well aligned between contractile groups of cells (73), creating an ECM architecture reminiscent of bridging fibrosis in the liver (32). The alignment of collagen fibrils enables long-range force transmission to propagate contractile signals much further than isotropic matrices (4, 84). Fibrotic matrices contain these highly anisotropic mechanical properties, likely produced from contractile cells.

Highly contractile myofibroblasts form the major fibrogenic cell, and the mechanosensitivity of myofibroblasts' ECM production has been implicated in the fibrosis of skin, muscle, lung, liver, and kidney (46). This positions the mechanosensing of matrix stiffness as a critical cog in the positive feedback loop that exists in fibroproliferative disorders (85). Further, myofibroblast contraction on stiff matrices also directly activates latent transforming growth factor-β, the primary profibrotic soluble factor, contributing additional positive feedback in fibrosis (86). The balance between ECM production and degradation is further set off balance by myofibroblast contraction because collagen fibrils under load are protected from degradation by matrix metalloproteinases (31). This "use it or lose it" mechanism makes existing scar tissues even more difficult to remodel.

As with other cells, myofibroblasts' mechanosensitivity to matrix stiffness relies upon the formation of contractile stress fibers anchored to the ECM through focal adhesions. Stress fiber formation has been modeled to highlight the sensitivity to applied stresses (60). The activation level, η, from 0 to 1 represents the proportion of polymerized actin and phosphorylated myosin within stress fibers following

$$\dot{\eta}(p) = [1 - \eta(p)]\frac{Ck_f}{\theta} - \left[1 - \frac{\sigma(p)}{\sigma_0(p)}\right]\eta(p)\frac{k_d}{\theta}, \qquad 2.$$

where p represents parameters for stress fiber position, time, and direction. The initiating pulse, given by $C = e^{-t_i/\theta}$, decays over time t_i, following the biomechanical or biochemical signal-inducing stress fiber formation. Rate constants k_f and k_d govern, respectively, rates of formation and dissociation of stress fibers. The constant θ controls the rate of decay of the inducing signal. The tension of the stress fiber is σ, and $\sigma_0 = \eta\sigma_{max}$ is the isometric tension at the current level of activation, η, relative to the maximum isometric tension of a fully activated stress fiber, σ_{max}. This leads to stress fiber formation that is proportional to the signal, but that follows an exponential decay. The kinetics of dissociation are tightly linked to the stress applied on the stress fibers, which are stable under isometric conditions, $\sigma(p) = \sigma_0(p)$. However, when contraction is permitted and, thus, the stress falls below the isometric condition, dissociation progresses. This highlights the role of focal adhesions in anchoring the cell on stiff matrices to allow for isometric contractions and sustained stress fiber formation (60). Within mature focal adhesions, α-actinin has been discovered to be a main link for the transmission of force between integrins and the cytoskeleton (66). How such intracellular structures are organized becomes the next question.

CYTOSKELETAL ORDER IN TERMS OF FORCE DIPOLES

Communication through deformation is mediated in part by cellular adhesions that couple the cytoskeleton to forces within a gel-like matrix or substrate (5, 70). Forces are generated in single cells by numerous actomyosin contractile units in nascent stress fibers in various cells, including stem cells, or sarcomeric units in muscle cells, and the forces are transmitted via the rest of the viscoelastic cytoskeleton and into the matrix. For beating cardiomyocytes, mechanical forces in the matrix due to mechanical probes or adjacent cells (59, 82) can result in changes in the phase

and frequency of beating (17). Cell motility has long been known to be regulated by substrate stiffness (as in durotaxis) (61), and cells can also attract or repel each other depending on substrate rigidity (68). Feedback occurring as resistance to force can lead to orientational order (34, 64, 90) or translational registry (21, 33, 55) that depends on matrix stiffness.

Forces exerted by one actomyosin contractile unit are equal and opposite, and hence dipolar so that they couple with the local strain due to other such units within the cell, which collectively contribute to the contractility of the cell and the elastic deformation of the matrix. The displacement in the matrix at position $\mathbf{r}'$ induced by a force dipole located at position $\mathbf{r}'$ is proportional to $1/|\mathbf{r}' - \mathbf{r}'|$ (49). Changes in matrix elastic energy depend on the orientation and distance between contractile units and give rise to matrix forces that act on cellular adhesions to move or reorient them. In the case of localized actomyosin forces, this can be written as the product of the distribution of these forces and the local displacement of the matrix in their vicinity. If the actomyosin units are modeled as force dipoles (comprising equal and opposite point forces separated by a distance that corresponds to the spacing of the two heads of a myosin II molecule), the matrix deformation energy is given by the product of each force dipole within the cell and the local strain (gradient of the displacement) due to the other force dipoles within the cell (34, 70). The theoretical approach is multiscale and can also be applied to entire cells, modeled as coarse-grained force dipoles, that interact via the matrix deformations due to adjacent contractile cells or other mechanical perturbations of the matrix or substrate.

For example, the force dipole for contractile units aligned along the z axis is written $p_{ij} = P\delta_{iz}\delta_{jz}$. In this simple case, both the force and separation vectors have the same orientation so there is only one component to the force dipole but, in general, there can be as many as nine components. As References 17 and 70 show, the deformation energy of the matrix accounts for the overlap of the strain fields of two nearby dipoles. This is equivalent to an effective interaction energy, H, which is the product of each dipole moment and the strain field induced by its counterpart:

$$H = \sum_{k \neq l} p_{ij}^k \varepsilon_{ij}^l. \qquad\qquad 3.$$

Here, p_{ij}^k and ε_{ij}^l are, respectively, the force dipole moment and the strain induced by the k-th and l-th dipoles. This is analogous to the interaction of an electric dipole with the local electric field in its immediate surrounding. For beating cells, these quantities can be time dependent, which changes the spatial decay of the strain induced by a force dipole that oscillates in time from a power law to an exponential (17). It is important to stress that this effective interaction of the neighboring dipoles is just a rewriting of the elastic energy of the matrix or substrate. Consequently, the force applied by the medium on a cellular adhesion can be written as a spatial derivative of the local elastic stress, which for a linear medium is proportional to the local strain. For example, the force applied to the adhesions along the z direction is (17, 33):

$$F_z = -p_{zz}^k \frac{\partial \varepsilon_{zz}^l}{\partial z}. \qquad\qquad 4.$$

Because the strain induced by a given actomyosin unit depends on the matrix or substrate elasticity, both the interaction energy as well as the force that acts on the other actomyosin units depend on the substrate elasticity. In general, the deformation-induced force decreases inversely with the elastic stiffness of the matrix. However, it has been shown experimentally that the magnitude of actomyosin contractility (which, in the theory, is related to the force dipole magnitude P) increases with stiffness almost linearly for soft substrates, and saturates for very rigid substrates (37). This arises from the biological adaptation of actomyosin contractility to the substrate or matrix stiffness and cannot be predicted from a purely mechanical point of view. The decreased strain and increased contractility (force dipole magnitude) with matrix stiffness

ultimately lead to the prediction of an optimal rigidity for which deformation-induced energies or forces are largest. This is a general feature of elastic interactions and is manifested experimentally in the existence of an optimal rigidity for both the orientational order (34, 64, 90) and translational registry order (21, 55) of actomyosin units within single cells.

NUCLEAR LINKAGES AND FORCES IN GENE REGULATION

Mechanical links between the ECM and the cytoskeleton can, in principle, transmit ECM-propagated forces to strain the nucleus and affect gene expression. Although integrins bind specific matrix proteins extracellularly, they link inside cells through focal adhesions to the actomyosin cytoskeleton. Myosin II is required for nearly all mechanisms of mechanotransduction, but all of the cytoskeletal elements—F-actin, microtubules, and intermediate filaments—can also connect to the nucleus. Nesprins span the outer nuclear membrane and can interact either directly with cytoskeletal elements or in complexes, which might be usefully viewed as nuclear analogs of focal adhesions. SUN protein trimers span the inner nuclear membrane and bind the lamins (20). Lamins are the primary component of the nuclear lamina, which establishes nuclear mechanical properties (48).

Direct physical links between the ECM and DNA can transduce signals, but there are numerous mechanosensitive signaling pathways that transmit stiffness signals to transcriptional machinery. One example is the Yes-associated protein (YAP) and transcriptional coactivator together with the PDZ binding motif (TAZ), which is often found in the cytosol of cells on soft matrices. In cells on a stiff matrix, YAP–TAZ translocates to the nucleus (27). Nuclear translocation occurs in short time scales of approximately 30 min when cells are placed on a stiff substrate. YAP–TAZ also retains the activated transcription factors SMAD2 and 3, which are key regulators of ECM genes (6). In contrast, NKX2.5 is a recently described mechanosensitive transcription factor that translocates from the nucleus to the cytoplasm when cells are on stiff substrates, but this occurs over the course of days (24). NKX2.5 translocation to the cytosol results in increased expression of α-SMA, a particularly responsive component of stress fibers. Thus, a prediction-based understanding of matrix mechanosensing requires modeling the rates of mechanosensitive pathways, as has been pursued for lamin A.

The strong positive scaling between nuclear lamin levels and tissue stiffness (**Figure 2b**) provides a suitably large dynamic range for insight and modeling. On the basis of in vitro studies of cells cultured on gels of controlled stiffness E, phosphorylation of lamin A in interphase nuclei is a key part of the underlying mechanosensitive gene circuit (10, 80). Low tension on the nucleus (on soft matrix or with myosin inhibition or detachment from plastic) allows access to lamin A of Ser and Thr kinase(s) in the CDK family (cyclin-dependent kinases). The likely mechanism is that the kinase is constant in concentration and activity, but the Ser and Thr sites in fibrous assemblies of lamin A become more accessible when the fibers are under low tension. This is similar to the use it or lose it mechanism for how proteases degrade collagen 1 fibers that are under low tension rather than high tension (67). For decades, it has been known that CDKs activated in cell division (especially CDK1) cause massive phosphorylation of both the A- and B-type lamins at many sites to solubilize them and uncage the chromatin for dividing the DNA between daughter cells; however, interphase phosphorylation occurs at approximately 10-fold lower levels and seems restricted to lamin A, and the phosphorylated lamin A often remains in the nucleus. Inhibitor studies implicate CDKs other than CDK1 (10). Phosphorylated lamin A is mobile in the nucleoplasm as shown in FRAP (fluorescence recovery after photobleaching) studies of phosphomimetic constructs of lamin A, and it also degrades faster than nonphosphorylated lamin A. Thus, soft matrix favors more phosphorylation and more degradation to minimize lamin A levels (**Figure 3a**).
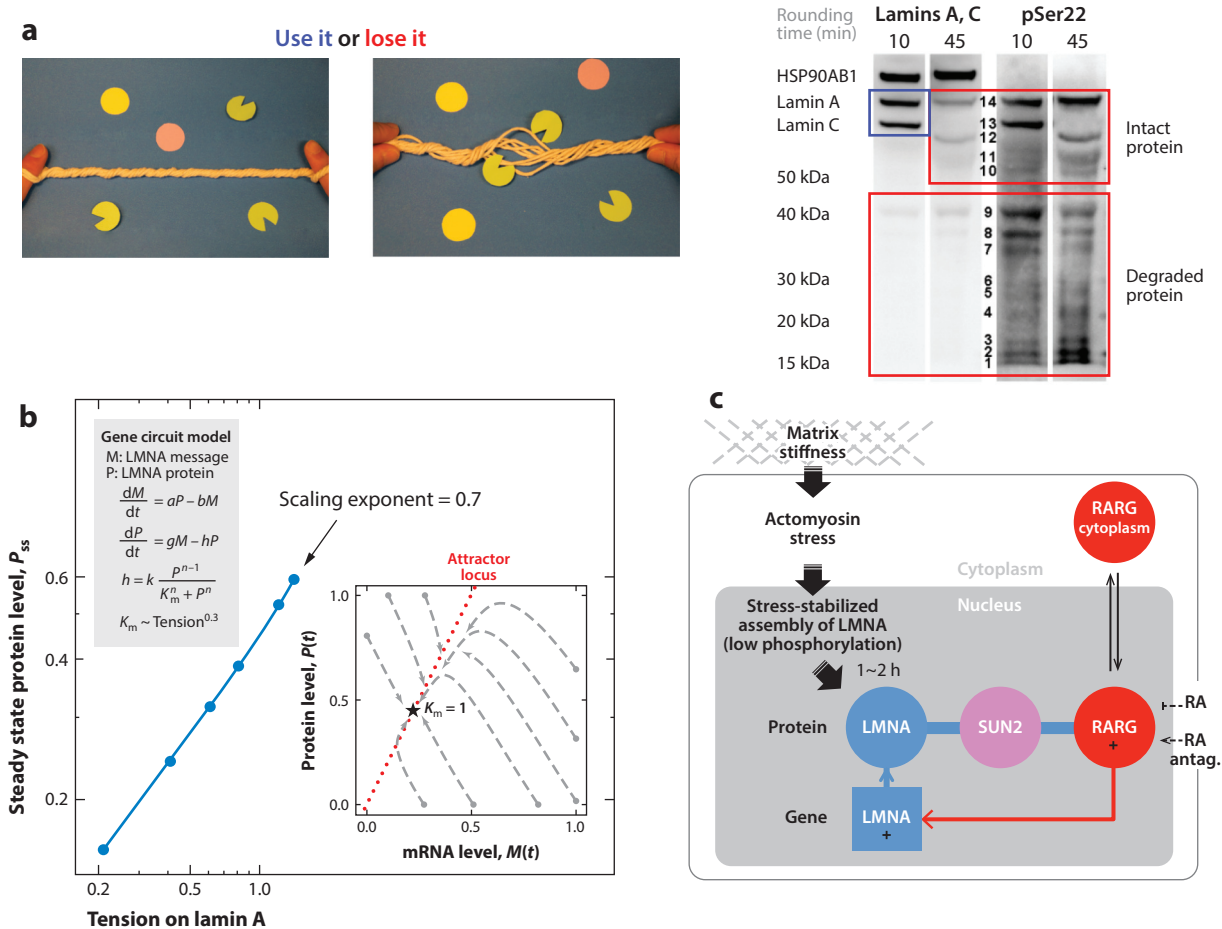
Figure 3

Tension on structural proteins can regulate their stability, which is sufficient to control gene expression. (*a*) Use it or lose it scheme of an intertwined filament under tension (*left*) or not (*right*) either excludes enzymatic activity or permits access. Immunoblots of lamins A and C show that the increased rounding time of a cell (10 min or 45 min) decreases the amount of intact protein and increases the amount of phosphorylated lamins A and C at phospho-Ser22 (pSer22) with low molecular weight (e.g., bands 1–4) (10). HSP90AB1 is a housekeeping protein. (*b*) The steady-state lamin A (LMNA) protein level scales with tension on lamin A filaments as a power law of 0.7 exponent. In the main plot, this result is calculated according to a model (*upper inset*) wherein the synthesis of message increases with protein, and protein degradation is suppressed by tension (24). In particular, the dissociation constant, K_m, of effective degradation weakens with tension. The lower inset shows the evolution to the steady state for a given value of tension. (*c*) Schematic of the mechanobiological gene circuit with details of the factors that couple lamin A protein to its transcription. When nuclear lamin A is high because the matrix is stiff and cytoskeletal stress on the nucleus is high, then lamin A binds SUN2, which helps retain the transcription factor RARG (retinoic acid receptor G) in the nucleus to drive the transcription of lamin A. This activity of RARG is modulated by soluble factors, retinoic acid (RA), and its antagonists.

Mechanoregulation of lamin A protein can occur in hours or less time, and it eventually feeds back into transcription of the lamin A gene (**Figure 3*b*,*c***) (80). The promoter region of lamin A (*LMNA*) harbors multiple retinoic acid response (RAR) elements that bind RAR transcription factors (evident in the ENCODE database; **https://www.encodeproject.org/**), and the immunoprecipitation of one RAR factor (RARG, retinoic acid receptor G) followed by mass spectrometry

identified the nuclear envelope protein SUN2 as a possible binding partner. SUN2 is an integral membrane protein known to bind lamin A protein, but SUN2 can also diffuse into the endoplasmic reticulum, contiguous with the nuclear envelope but extended into much of the cytoplasm. Nuclear entry of RARG proved to be partially regulated by the levels of both SUN2 and lamin A. This example of a mechanobiological gene circuit is perhaps a first and can be formalized mathematically as (80)

$$\text{d(lamin A)}/\text{d}t = a\ LMNA - \text{(tension-suppressed degradation)},$$
$$\text{d}LMNA/\text{d}t = b\,\text{(lamin A)} - c\ LMNA,$$

where a, b, and c are constants, and the tension-suppressed degradation term exhibits Michaelis–Menten kinetics with lamin A. For the tension-suppressed degradation term, the model assumes the binding affinity K_m (μM) for lamin A fibers to the rate-limiting enzyme (CDK kinase and/or the protease) is suppressed by tension on the fibers according to a power law K_m (μM) $\sim$ tension$^{\alpha}$. This could happen because tension slows the association rate (e.g., binding site is a loop that is straightened by tension) and/or because tension accelerates dissociation (i.e., kinase pops off). Steady-state solutions show that lamin A protein increases as a function of tension (for $\alpha = 0.3$) or, equivalently, as a function of matrix stiffness because tension on the nucleus increases with the stiffness of the matrix. The soluble microenvironment co-modulates the nuclear mechanosensing of matrix mechanics because RAR is, of course, regulated by retinoic acid, which is a membrane-permeable lipophilic molecule derived from vitamin A and is essential in development and differentiation (65).

MATRIX MECHANOSENSING BY STEM CELLS IN REGENERATIVE MEDICINE

Efforts to repair, regenerate, or replace living tissues seem likely to benefit from engineered microenvironments that instruct the behaviors of cells, particularly stem cells. Such cells are capable of differentiating into various cell types of the body as well as reproducing more stem cells via self-renewal. Such stem cell fates have traditionally been controlled via soluble growth factors and small molecules (such as retinoic acid) that regulate signaling pathways (39), but it is also becoming increasingly important to consider the mechanical properties of engineered microenvironments as another key regulator of stem cell differentiation. Indeed, previous work in which mesenchymal stem cells (MSCs) were cultured atop collagen 1–modified polyacrylamide gels that mimic the tissue elasticity of neural tissue, muscle tissue, or developing bone provided the first compelling evidence that matrix elasticity can help direct stem cell fate (30). Not only did MSCs express markers for neural, muscle, or bone cells when grown on gels of corresponding stiffness, but when their myosin II–based mechanical interactions with the matrix were inhibited, expression and/or localization of lineage specification markers was also interrupted. Importantly, myosin II affects cell morphology and cytoskeleton within hours of a cell contacting a substrate, whereas evident expression changes take days, which indicates a separation of time scales. This work has been extended to show that beyond purely elastic substrates, the viscous components of viscoelastic materials also influence MSC differentiation (12). Gels with a high viscous component promoted differentiation toward a smooth muscle cell lineage, with increased motility and lamellipodial protrusion.

Some adult tissues are truly regenerated in 2D processes, such as adult bone in which osteoblasts on top of a bone surface deposit a layer of matrix (osteoid) that is then mineralized in a process of epitaxial growth (30). However, for other tissues (e.g., brain), 2D cultures can provide only reductionist insight into factors that could be important to 3D tissue biology. Insights into the

regeneration of 3D tissues could benefit from rationally engineered 3D culture systems that (*a*) eliminate apical–basal polarization while still paying attention to (*b*) access to soluble nutrients and (*c*) physical caging constraints on cell morphology or proliferation, or both. The encapsulation of MSCs in 3D hydrogels of alginate (a carbohydrate commonly derived from brown seaweed) that was modified with Arg–Gly–Asp (or RGD) adhesion peptides (40) showed that soft gels with elasticity from 2.5 to 5 kPa favored adipogenesis (a soft tissue lineage), whereas stiff gels of 11 to 30 kPa favored osteogenesis. Although 2D cultures on these gels were not studied and would allow one to measure any changes in gel mechanics caused by cells, the results are in close agreement with earlier 2D studies that used nondegradable polyacrylamide gels (80). Any degradation or extensive physical remodeling of the matrix can be expected to change the matrix mechanics and, therefore, requires local measurements of the mechanics of the gel around the cell. The encapsulation of MSCs in 3D hyaluronic acid–based gels indeed revealed that when the cell-mediated degradation of stiff gels was restricted so that cells remained spherically encaged, upregulation of myosin II tension was required to favor osteogenesis over adipogenesis (45). This is consistent with the theory and experiments on MSCs that showed how cell shape influences cytoskeletal tension (90).

Matrix mechanotransduction pathways that affect stem cell fate must somehow enter the nucleus and coregulate gene expression. Such pathways could involve the nuclear accumulation and autocatalytic expression of basal levels of lineage-specific transcription factors (30) or perhaps more generic factors. YAP and TAZ are well-characterized examples of transcriptional regulators that generally affect cell growth and differentiation. Human pluripotent stem cells (hPSCs) cultured on brain-like compliant polyacrylamide hydrogel (0.75 kPa elasticity) showed nuclear exclusion of YAP and differentiation into postmitotic neurons, whereas hPSCs on stiff gels (10 kPa) showed abundant YAP nuclear localization and maintenance of pluripotency (58). Compared with traditional neurogenic induction methods that use soluble factors, hPSCs more rapidly and efficiently differentiated into neurons on the compliant gels in the absence of neurogenic induction factors. Furthermore, dynamic changes in substrate stiffness have highlighted an important window of mechanosensitivity in stem cell neuronal differentiation (63). However, the results for hPSCs on the stiff gels indicate differences from MSCs, which highlights the cell type–specific nature of mechanoresponses. Indeed, hematopoietic stem and progenitor cells taken from marrow, which is soft in this respect and similar to brain tissue, or else taken from a stiffer bone niche are also mechanoresponsive to matrix elasticity, but these cells remain blood-lineage committed (75).

Tissues and gels can, of course, possess mechanical properties far more complex than simple elasticity. If they experience too much strain or stress, they will yield, break, and/or flow. Some tissues, such as embryonic brain, are so soft that they creep and flow irreversibly (exhibiting plasticity) under microscale strain, whereas other tissues, such as embryonic heart, are resiliently elastic and recover completely from externally imposed strain (54). Bulk measurements of a few tissues of intermediate stiffness, such as liver, have also indicated that these tissues exhibit stress relaxation when exposed to what might be a nonphysiologically high strain of 15% (14). This has motivated the development of alginate gels with tunable stress relaxation timescales (1 min to 40 min) but otherwise equivalent elastic moduli, ligand densities, and degradation characteristics (14). MSCs grown in 9 kPa gels exhibited maximum adipogenesis in slow-relaxing gels, but MSCs grown in 17 kPa gels exhibited maximum osteogenesis in fast-relaxing gels. Adhesive ligand clustering was also measured and could relate to the accumulation of gel around a cell—hence locally stiff matrix— but it is also clear that matrix relaxation permits cell protrusion and morphological changes so that cell shape can again influence cytoskeletal tension (90). Matrix relaxation can also permit proliferation that can modulate differentiation. Although the heterogeneous mechanics that arise after cell integration requires careful measurement, these studies nevertheless underscore the fundamental roles that matrix mechanics and physical properties have on stem cell fate.

Matrix elasticity in vitro clearly influences transplantation in vivo. In particular, the self-renewal of proliferating stem cells is influenced by matrix elasticity, at least for mouse muscle stem cells (38). The growth of freshly isolated cells on muscle-like 12 kPa hydrogels (functionalized with the ECM protein laminin) produced the greatest number of viable, transplant-competent cells compared with softer or stiffer gels or even 2D culture plastic (approximately 10^6 kPa stiffness) coated with a very thin layer of gel to maintain the surface chemistry. A memory of in vitro matrix interactions was demonstrated with MSCs derived from bone marrow (which is soft) and then cultured on rigid polystyrene dishes for a prolonged time, which thereby favored osteogenesis even when the cells were transferred to a 2 kPa polyethylene glycol (PEG) hydrogel (88). Alternatively, if culture on plastic is kept sufficiently brief, then such differentiation can be suppressed.

Ensuring that a matrix is sufficiently malleable to cells can facilitate wound healing in vivo. Indeed, the myosin-dependent contraction and migration of fibroblasts around a wound gap are primary mechanisms through which closure occurs, as opposed to the proliferation of cells (69). The forces transmitted through cell–cell contacts have proven to be critical factors in layers of cells moving together, as in wound healing (81). Using void-forming alginate hydrogels, murine MSCs exhibited the greatest proliferation, collagen deposition, and mineralization, with construct elasticity ranging from 20 to 60 kPa (41). Transplantation into a bone defect model showed maximal tissue regeneration with gels in the intermediate range of stiffness, perhaps similar in stiffness to precalcified bone, or osteoid. More in-depth analysis is needed as other mechanisms, such as host cell infiltration and material degradation, could impact the response. The formation of epithelial cysts also exhibits maximum polarization and lumen formation in a narrow range of ECM elasticity when using PEG hydrogels, with abnormal morphogenesis observed for softer and stiffer gels (28). It seems that a matrix must be sufficiently rigid to provide appropriate cues to cells yet compliant enough to allow a given cell type—that might be strong or might be weak—to manipulate the matrix for migration, spreading, and proliferation. Adhesive ligand density is generally important for cells to engage the matrix, and also for both adhesion and protease degradation of ECM-regulated apical–basal polarity and lumenogenesis. Thus, synthetic ECM technologies can provide insight into ECM regulation of complex morphogenetic behaviors and provide potentially useful rules for regenerative medicine.

Reprogramming the epigenetic state of primary mouse fibroblasts to induced pluripotent stem cells (iPSCs) has also been examined in 3D synthetic hydrogels with modulation of matrix stiffness, degradability, and ligand (11). Using PEG hydrogels conjugated with adhesive peptides and cross-linked with matrix metalloproteinase-cleavable peptides, the fibroblasts were encapsulated and transduced with the four traditional Yamanaka factors. Compared with traditional reprogramming in polystyrene dishes, the gels supported sustained proliferation and accelerated the reprogramming of the somatic cells. Compared with 128 microenvironmental conditions spanning stiffness, biochemical presentation, and degradation, the highest efficiency of iPSC reprogramming was achieved with hydrogels having a stiffness of 600 Pa, high degradability, and functionalization with epithelial cell adhesion molecule (EpCAM). Matrigel (Corning, New York, NY) produced similar efficiency but with less homogeneity in induction, which is interesting in that Matrigel lacks EpCAM but is similarly soft, which mimics embryonic tissue.

CONCLUSIONS: FROM THE EPIGENETICS OF MECHANOSENSING TO THE MECHANOGENOMICS OF CANCER

The above discussions often pertain to epigenetics in the sense that the genome is invariant as expression varies with the mechanics of matrix and tissue. Epigenetics involves many layers of gene expression regulation that have not yet been examined in relation to matrix mechanosensing,

such as methylation of DNA, histone modification, and spatial organization of chromosomes. The detailed biochemical kinetics of any changes in such increasingly established processes will require careful comparisons to the rapid kinetics of cytoskeletal changes (hours), but suitably chosen tissues should also be used to calibrate the epigenetic fine tuning of gene expression. For this reason among many others, we began this review by recognizing that tissues and their constituent matrices and cells are built from polymers with tissue-dependent concentrations (i.e., epigenetically set levels). Standardized public transcriptome data together with mass spectrometry proteomics data and tissue stiffness measurements were then used to illustrate polymer physics–type scaling for the most abundant protein in tissue and collagen 1, as well as for one of the most abundant nuclear structural proteins, lamin A. Transcriptome data were discussed not only for hearts from a wide range of species, which indicates common epigenetic pathways despite different genomes, but also for all sorts of perturbations to try to highlight universality in scaling. Injury, including chronic disease, was briefly reviewed because it almost invariably leads to fibrosis defined by increased collagen and/or cross-linking as well as altered tissue mechanics and function.
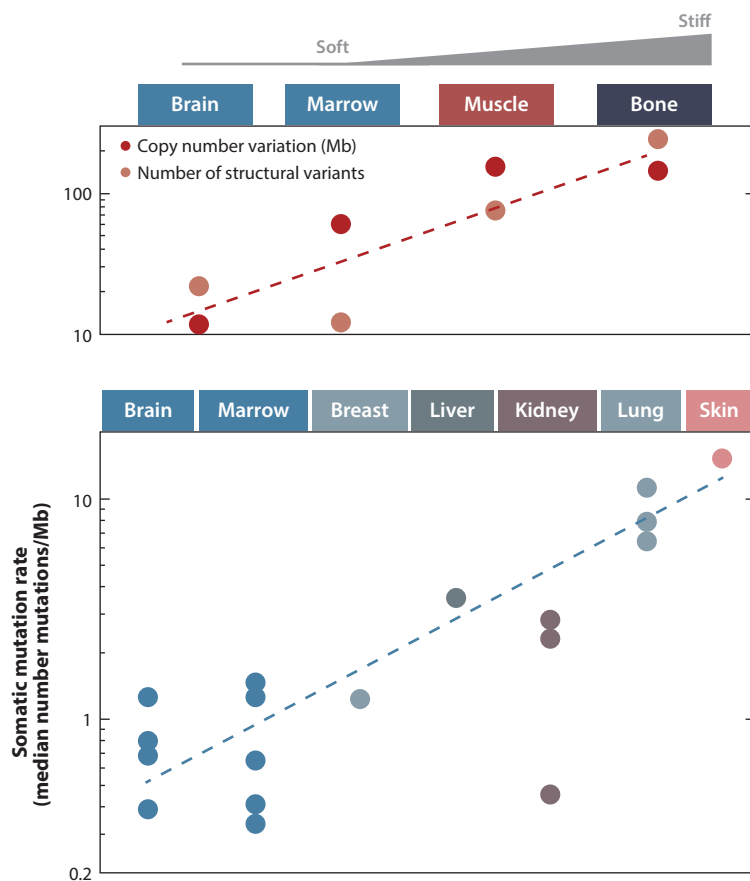
Figure 4

Cancer genome mutations seem to increase with tissue stiffness. Public data sets of chromosome-level changes, such as chromosome copy number variations in units of megabases (Mb) of DNA, seem lowest in soft tissues, such as brain and marrow, compared with cancers in bone (15). A similar trend is evident for somatic mutations (per megabase of DNA) (1), with different colors used for tumors in the different tissues.

However, tissues are complex, which makes it difficult to distinguish coincidental correlations in tissues from cell-level mechanisms.

Numerous culture systems using various materials of controlled elasticity and separately controlled biochemistry (from adhesive ligand to soluble factors) were reviewed as influencing isolated cells in terms of morphology and cytoskeleton, on short time scales, and also in terms of expression levels and even differentiation of stem cells on longer time scales. The reductionist approaches in culture can certainly be relevant to tissue engineering as well as the basic science of development, but they also parse the independent variables sufficiently to enable theoretical physics approaches. Theory serves as always to formalize assumptions in fitting experimental results and in generating predictions for the next experiments. It has been particularly successful in modeling the organization of actomyosin cytoskeleton force dipoles in response to matrix elasticity, demonstrating that soft matrices suppress order as observed in experiments. Simpler scalar descriptions of stresses were also integrated into otherwise conventional equations for regulation of gene and protein concentrations, with calculations ultimately showing that actomyosin stress that increases with matrix stiffness tends to stabilize and thereby increase lamin A. Despite advances in our understanding, much more work is needed on the epigenetic mechanisms of matrix mechanosensing.

In cancer, the genomes of tumors have changed and likely continue to change, with large-scale sequencing (1, 15) revealing the extent of such changes, and, remarkably, genome changes in cancer trend again with tissue stiffness (**Figure 4**). Stiff tissues, such as bone, muscle, and even skin, lead to cancers that exhibit more genomic changes than tumors originating in soft tissues, such as brain and marrow. Even for skin cancer in which ultraviolet radiation (particularly with aging) clearly accounts for many or most mutations (56), changes in chromosome copy number associate with tumor stiffness, with point mutations increasing more weakly as all genomic changes reach a maximum in invasive melanoma (71). Epithelial tissues tend to be moderately stiff as part of a barrier function that also exposes them to carcinogens, but carcinogens cannot easily explain the increases in chromosome copy number, from low rates in soft marrow and brain to elevated rates in stiff muscle and higher rates in rigid bone.

Mutations can result from DNA damage and so the scaling of mutation rate with tissue stiffness is likely explained by mechanoregulation of key DNA damage or repair processes, or both. Nuclear localization of DNA repair factors is indeed emerging as mechanosensitive (42, 43), although many aspects of the mechanism(s) must still be addressed. The cancer genome data viewed from this mechanobiological perspective nonetheless suggest there are some underlying processes of matrix mechanosensing by factors that can alter the fundamental sequence of the genome in cells—that is, a new field of mechanogenomics.

DISCLOSURE STATEMENT

ACKNOWLEDGMENTS

LITERATURE CITED

1. Alexandrov LB, Nik-Zainal S, Wedge DC, Aparicio SA, Behjati S, et al. 2013. Signatures of mutational processes in human cancer. *Nature* 500:415–21

2. Barrett T, Wilhite SE, Ledoux P, Evangelista C, Kim IF, et al. 2013. NCBI GEO: Archive for functional genomics data sets—update. *Nucleic Acids Res*. 41:D991–95

3. Barry-Hamilton V, Spangler R, Marshall D, McCauley S, Rodriguez HM, et al. 2010. Allosteric inhibition of lysyl oxidase-like-2 impedes the development of a pathologic microenvironment. *Nat. Med.* 16:1009–17

4. Bates JH, Davis GS, Majumdar A, Butnor KJ, Suki B. 2007. Linking parenchymal disease progression to changes in lung mechanical function by percolation. *Am. J. Respir. Crit. Care Med.* 176:617–23

5. Ben-Yaakov D, Golkov R, Shokef Y, Safran SA. 2015. Response of adherent cells to mechanical perturbations of the surrounding matrix. *Soft Matter* 11:1412–24

6. Beyer TA, Weiss A, Khomchuk Y, Huang K, Ogunjimi AA, et al. 2013. Switch enhancers interpret TGF-β and Hippo signaling to control cell fate in human embryonic stem cells. *Cell Rep*. 5:1611–24

7. Bisping E, Ikeda S, Kong SW, Tarnavski O, Bodyak N, et al. 2006. Gata4 is required for maintenance of postnatal cardiac function and protection from pressure overload–induced heart failure. *PNAS* 103:14471–76

8. Booth AJ, Hadley R, Cornett AM, Dreffs AA, Matthes SA, et al. 2012. Acellular normal and fibrotic human lung matrices as a culture system for in vitro investigation. *Am. J. Respir. Crit. Care Med.* 186:866–76

9. Buxboim A, Rajagopal K, Brown AE, Discher DE. 2010. How deeply cells feel: methods for thin gels. *J. Phys. Condens. Matter* 22:194116

10. Buxboim A, Swift J, Irianto J, Spinler KR, Dingal PC, et al. 2014. Matrix elasticity regulates lamin-A,C phosphorylation and turnover with feedback to actomyosin. *Curr. Biol.* 24:1909–17

11. Caiazzo M, Okawa Y, Ranga A, Piersigilli A, Tabata Y, Lutolf MP. 2016. Defined three-dimensional microenvironments boost induction of pluripotency. *Nat. Mater.* 15:344–52

12. Cameron AR, Frith JE, Gomez GA, Yap AS, Cooper-White JJ. 2014. The effect of time-dependent deformation of viscoelastic hydrogels on myogenic induction and Rac1 activity in mesenchymal stem cells. *Biomaterials* 35:1857–68

13. Carver W, Goldsmith EC. 2013. Regulation of tissue fibrosis by the biomechanical environment. *BioMed Res. Int*. 2013:101979

14. Chaudhuri O, Gu L, Klumpers D, Darnell M, Bencherif SA, et al. 2016. Hydrogels with tunable stress relaxation regulate stem cell fate and activity. *Nat. Mater.* 15:326–34

15. Chen X, Bahrami A, Pappo A, Easton J, Dalton J, et al. 2014. Recurrent somatic structural variations contribute to tumorigenesis in pediatric osteosarcoma. *Cell Rep.* 7:104–12

16. Cho S, Irianto J, Discher DE. 2017. Mechanosensing by the nucleus: from pathways to scaling relationships. *J. Cell Biol.* 216:305–15

17. Cohen O, Safran SA. 2016. Elastic interactions synchronize beating in cardiomyocytes. *Soft Matter* 12:6088–95

18. Cool CD, Groshong SD, Rai PR, Henson PM, Stewart JS, Brown KK. 2006. Fibroblast foci are not discrete sites of lung injury or repair: the fibroblast reticulum. *Am. J. Respir. Crit. Care Med.* 174:654–58

19. Cox TR, Erler JT. 2011. Remodeling and homeostasis of the extracellular matrix: implications for fibrotic diseases and cancer. *Dis. Model. Mech.* 4:165–78

20. Crisp M, Liu Q, Roux K, Rattner JB, Shanahan C, et al. 2006. Coupling of the nucleus and cytoplasm: role of the LINC complex. *J. Cell Biol.* 172:41–53

21. Dasbiswas K, Majkut S, Discher DE, Safran SA. 2015. Substrate stiffness–modulated registry phase correlations in cardiomyocytes map structural order to coherent beating. *Nat. Commun.* 6:6085

22. Degos F, Perez P, Roche B, Mahmoudi A, Asselineau J, et al. 2010. Diagnostic accuracy of FibroScan and comparison to liver fibrosis biomarkers in chronic viral hepatitis: a multicenter prospective study (the FIBROSTIC study). *J. Hepatol.* 53:1013–21

23. Delgado-Olguin P, Huang Y, Li X, Christodoulou D, Seidman CE, et al. 2012. Epigenetic repression of cardiac progenitor gene expression by Ezh2 is required for postnatal cardiac homeostasis. *Nat. Genet.* 44:343–47

24. Dingal PC, Bradshaw AM, Cho S, Raab M, Buxboim A, et al. 2015. Fractal heterogeneity in minimal matrix models of scars modulates stiff-niche stem-cell responses via nuclear exit of a mechanorepressor. *Nat. Mater.* 14:951–60

25. Discher DE, Mooney DJ, Zandstra PW. 2009. Growth factors, matrices, and forces combine and control stem cells. *Science* 324:1673–77

26. Dittmer TA, Misteli T. 2011. The lamin protein family. *Genome Biol.* 12:222

27. Dupont S, Morsut L, Aragona M, Enzo E, Giulitti S, et al. 2011. Role of YAP/TAZ in mechanotransduction. *Nature* 474:179–83

28. Enemchukwu NO, Cruz-Acuna R, Bongiorno T, Johnson CT, Garcia JR, et al. 2016. Synthetic matrices reveal contributions of ECM biophysical and biochemical properties to epithelial morphogenesis. *J. Cell Biol.* 212:113–24

29. Engler A, Bacakova L, Newman C, Hategan A, Griffin M, Discher D. 2004. Substrate compliance versus ligand density in cell on gel responses. *Biophys. J.* 86:617–28

30. Engler AJ, Sen S, Sweeney HL, Discher DE. 2006. Matrix elasticity directs stem cell lineage specification. *Cell* 126:677–89

31. Flynn BP, Bhole AP, Saeidi N, Liles M, Dimarzio CA, Ruberti JW. 2010. Mechanical strain stabilizes reconstituted collagen fibrils against enzymatic degradation by mammalian collagenase matrix metalloproteinase 8 (MMP-8). *PLOS ONE* 5:e12337

32. Fontana RJ, Goodman ZD, Dienstag JL, Bonkovsky HL, Naishadham D, et al. 2008. Relationship of serum fibrosis markers with liver fibrosis stage and collagen content in patients with advanced chronic hepatitis C. *Hepatology* 47:789–98

33. Friedrich BM, Buxboim A, Discher DE, Safran SA. 2011. Striated acto-myosin fibers can reorganize and register in response to elastic interactions with the matrix. *Biophys. J.* 100:2706–15

34. Friedrich BM, Safran SA. 2012. How cells feel their substrate: spontaneous symmetry breaking of active surface stresses. *Soft Matter* 8:3223–30

35. Frisch SM, Screaton RA. 2001. Anoikis mechanisms. *Curr. Opin. Cell Biol.* 13:555–62

36. Gennes P-G. 1979. *Scaling Concepts in Polymer Physics*. Ithaca, NY: Cornell Univ. Press

37. Ghibaudo M, Saez A, Trichet L, Xayaphoummine A, Browaeys J, et al. 2008. Traction forces and rigidity sensing regulate cell functions. *Soft Matter* 4:1836–43

38. Gilbert PM, Havenstrite KL, Magnusson KE, Sacco A, Leonardi NA, et al. 2010. Substrate elasticity regulates skeletal muscle stem cell self-renewal in culture. *Science* 329:1078–81

39. Guilak F, Cohen DM, Estes BT, Gimble JM, Liedtke W, Chen CS. 2009. Control of stem cell fate by physical interactions with the extracellular matrix. *Cell Stem Cell* 5:17–26

40. Huebsch N, Arany PR, Mao AS, Shvartsman D, Ali OA, et al. 2010. Harnessing traction-mediated manipulation of the cell/matrix interface to control stem-cell fate. *Nat. Mater.* 9:518–26

41. Huebsch N, Lippens E, Lee K, Mehta M, Koshy ST, et al. 2015. Matrix elasticity of void-forming hydrogels controls transplanted-stem-cell-mediated bone formation. *Nat. Mater.* 14:1269–77

42. Irianto J, Pfeifer CR, Bennett RR, Xia Y, Ivanovska IL, Liu AJ, et al. 2016. Nuclear constriction segregates mobile nuclear proteins away from chromatin. *Mol. Biol. Cell* 27:401–20

43. Irianto J, Xia Y, Pfeifer CR, Athirasala A, Ji J, et al. 2017. DNA damage follows repair factor depletion and portends genome variation in cancer cells after pore migration. *Curr. Biol.* 27:210–23

44. Jorba I, Uriarte JJ, Campillo N, Farre R, Navajas D. 2017. Probing micromechanical properties of the extracellular matrix of soft tissues by atomic force microscopy. *J. Cell. Physiol.* 232:19–26

45. Khetan S, Guvendiren M, Legant WR, Cohen DM, Chen CS, Burdick JA. 2013. Degradation-mediated cellular traction directs stem cell fate in covalently crosslinked three-dimensional hydrogels. *Nat. Mater.* 12:458–65

46. Klingberg F, Hinz B, White ES. 2013. The myofibroblast matrix: implications for tissue repair and fibrosis. *J. Pathol.* 229:298–309

47. Korsmo MJ, Ebrahimi B, Eirin A, Woollard JR, Krier JD, et al. 2013. Magnetic resonance elastography noninvasively detects in vivo renal medullary fibrosis secondary to swine renal artery stenosis. *Investig. Radiol.* 48:61–68

48. Lammerding J, Fong LG, Ji JY, Reue K, Stewart CL, et al. 2006. Lamins A and C but not lamin B1 regulate nuclear mechanics. *J. Biol. Chem.* 281:25768–80

49. Landau L, Lifshitz E. 1970. *Theory of Elasticity*. Oxford, UK: Pergamon Press

50. Levental KR, Yu H, Kass L, Lakins JN, Egeblad M, et al. 2009. Matrix crosslinking forces tumor progression by enhancing integrin signaling. *Cell* 139:891–906

51. Licup AJ, Munster S, Sharma A, Sheinman M, Jawerth LM, et al. 2015. Stress controls the mechanics of collagen networks. *PNAS* 112:9573–78

52. Liu F, Mih JD, Shea BS, Kho AT, Sharif AS, et al. 2010. Feedback amplification of fibrosis through matrix stiffening and COX-2 suppression. *J. Cell Biol.* 190:693–706

53. Lopez B, Querejeta R, Gonzalez A, Larman M, Diez J. 2012. Collagen cross-linking but not collagen amount associates with elevated filling pressures in hypertensive patients with stage C heart failure: potential role of lysyl oxidase. *Hypertension* 60:677–83

54. Majkut S, Dingal PC, Discher DE. 2014. Stress sensitivity and mechanotransduction during heart development. *Curr. Biol.* 24:R495–501

55. Majkut S, Idema T, Swift J, Krieger C, Liu A, Discher DE. 2013. Heart-specific stiffening in early embryos parallels matrix and myosin expression to optimize beating. *Curr. Biol.* 23:2434–39

56. Martincorena I, Roshan A, Gerstung M, Ellis P, Van Loo P, et al. 2015. Tumor evolution: high burden and pervasive positive selection of somatic mutations in normal human skin. *Science* 348:880–86

57. McKee CT, Last JA, Russell P, Murphy CJ. 2011. Indentation versus tensile measurements of Young's modulus for soft biological tissues. *Tissue Eng. Part B Rev.* 17:155–64

58. Musah S, Wrighton PJ, Zaltsman Y, Zhong X, Zorn S, et al. 2014. Substratum-induced differentiation of human pluripotent stem cells reveals the coactivator YAP is a potent regulator of neuronal specification. *PNAS* 111:13805–10

59. Nitsan I, Drori S, Lewis YE, Cohen S, Tzlil S. 2016. Mechanical communication in cardiac cell synchronized beating. *Nat. Phys.* 12:472–77

60. Pathak A, Deshpande VS, McMeeking RM, Evans AG. 2008. The simulation of stress fibre and focal adhesion development in cells on patterned substrates. *J. R. Soc. Interface* 5:507–24

61. Pelham RJ Jr., Wang Y. 1997. Cell locomotion and focal adhesions are regulated by substrate flexibility. *PNAS* 94:13661–65

62. Rajan S, Williams SS, Jagatheesan G, Ahmed RP, Fuller-Bicer G, et al. 2006. Microarray analysis of gene expression during early stages of mild and severe cardiac hypertrophy. *Physiol. Genom.* 27:309–17

63. Rammensee S, Kang MS, Georgiou K, Kumar S, Schaffer DV. 2017. Dynamics of mechanosensitive neural stem cell differentiation. *Stem Cells* 35:497–506

64. Rehfeldt F, Brown AE, Raab M, Cai S, Zajac AL, et al. 2012. Hyaluronic acid matrices show matrix stiffness in 2D and 3D dictates cytoskeletal order and myosin-II phosphorylation within stem cells. *Integr. Biol.* 4:422–30

65. Rhinn M, Dolle P. 2012. Retinoic acid signalling during development. *Development* 139:843–58

66. Roca-Cusachs P, del Rio A, Puklin-Faucher E, Gauthier NC, Biais N, Sheetz MP. 2013. Integrin-dependent force transmission to the extracellular matrix by α-actinin triggers adhesion maturation. *PNAS* 110:E1361–70

67. Ruberti JW, Hallab NJ. 2005. Strain-controlled enzymatic cleavage of collagen in loaded matrix. *Biochem. Biophys. Res. Commun.* 336:483–89

68. Ryan J, Perez-Avila CA, Vaughan N. 1995. Insulin dependent diabetes mellitus and deliberate self-harm. *J. Accid. Emerg. Med.* 12:296–97

69. Sakar MS, Eyckmans J, Pieters R, Eberli D, Nelson BJ, Chen CS. 2016. Cellular forces and matrix assembly coordinate fibrous tissue repair. *Nat. Commun.* 7:11036

70. Schwarz US, Safran SA. 2013. Physics of adherent cells. *Rev. Mod. Phys.* 85:1327

71. Shain AH, Yeh I, Kovalyshyn I, Sriharan A, Talevich E, et al. 2015. The genetic evolution of melanoma from precursor lesions. *N. Engl. J. Med.* 373:1926–36

72. Sharma A, Licup AJ, Jansen KA, Rens R, Sheinman M, Koenderink GH. 2016. Strain-controlled criticality governs the nonlinear mechanics of fibre networks. *Nat. Phys.* 12:584–87

73. Shi Q, Ghosh RP, Engelke H, Rycroft CH, Cassereau L, et al. 2014. Rapid disorganization of mechanically interacting systems of mammary acini. *PNAS* 111:658–63

74. Shin JW, Swift J, Spinler KR, Discher DE. 2011. Myosin-II inhibition and soft 2D matrix maximize multinucleation and cellular projections typical of platelet-producing megakaryocytes. *PNAS* 108:11458–63

75. Shin JW, Buxboim A, Spinler KR, Swift J, Christian DA, et al. 2014. Contractile forces sustain and polarize hematopoiesis from stem and progenitor cells. *Cell Stem Cell* 14:81–93

76. Smith LR, Barton ER. 2014. Collagen content does not alter the passive mechanical properties of fibrotic skeletal muscle in *mdx* mice. *Am. J. Physiol. Cell Physiol.* 306:C889–98

77. Smith LR, Hammers DW, Sweeney HL, Barton ER. 2015. Increased collagen cross-linking is a signature of dystrophin-deficient muscle. *Muscle Nerve* 54:71–78

78. Smith LR, Lee KS, Ward SR, Chambers HG, Lieber RL. 2011. Hamstring contractures in children with spastic cerebral palsy result from a stiffer ECM and increased in vivo sarcomere length. *J. Physiol.* 589:2625–39

79. Sonna LA, Fujita J, Gaffin SL, Lilly CM. 2002. Effects of heat and cold stress on mammalian gene expression. *J. Appl. Physiol.* 92:1725–42

80. Swift J, Ivanovska IL, Buxboim A, Harada T, Dingal PC, et al. 2013. Nuclear lamin-A scales with tissue stiffness and enhances matrix-directed differentiation. *Science* 341:1240104

81. Tambe DT, Hardin CC, Angelini TE, Rajendran K, Park CY, et al. 2011. Collective cell guidance by cooperative intercellular forces. *Nat. Mater.* 10:469–75

82. Tang X, Bajaj P, Bashir R. 2016. How far cardiac cells can see each other mechanically. *Soft Matter* 7:6151–58

83. Vizcaino JA, Csordas A, del-Toro N, Dianes JA, Griss J, et al. 2016. 2016 update of the PRIDE database and its related tools. *Nucleic Acids Res.* 44:D447–56

84. Wang H, Abhilash AS, Chen CS, Wells RG, Shenoy VB. 2014. Long-range force transmission in fibrous matrices enabled by tension-driven alignment of fibers. *Biophys. J.* 107:2592–603

85. Wells RG. 2013. Tissue mechanics and fibrosis. *Biochim. Biophys. Acta* 1832:884–90

86. Wipff PJ, Rifkin DB, Meister JJ, Hinz B. 2007. Myofibroblast contraction activates latent TGF-β1 from the extracellular matrix. *J. Cell Biol.* 179:1311–23

87. Wynn TA. 2007. Common and unique mechanisms regulate fibrosis in various fibroproliferative diseases. *J. Clin. Investig.* 117:524–29

88. Yang C, Tibbitt MW, Basta L, Anseth KS. 2014. Mechanical memory and dosing influence stem cell fate. *Nat. Mater.* 13:645–52

89. Yang YL, Leone LM, Kaufman LJ. 2009. Elastic moduli of collagen gels can be predicted from two-dimensional confocal microscopy. *Biophys. J.* 97:2051–60

90. Zemel A, Rehfeldt F, Brown AE, Discher DE, Safran SA. 2010. Optimal matrix rigidity for stress fiber polarization in stem cells. *Nat. Phys.* 6:468–73